Antarct. Meteorite Res., **11**, 189–201, 1998

CHARACTERISTICS OF NATURAL REMANENT MAGNETIZATION OF NOVA PETRÓPOLIS IRON METEORITE (II)

Minoru FUNAKI[1] and Jacques DANON[2]*

[1]*National Institute of Polar Researh, 9–10, Kaga 1-chome, Itabashi-ku, Tokyo 173-8515*
[2]*Centro Brasileiro de Pesquisas Fisicas, Rua Dr. Xavier Sigaud, 150 22290-180 Rio de Janeiro, RJ Brasil*

Abstract: Nova Petrópolis (medium octahedrite, IIIA) was studied magnetically focusing on the acquisition mechanism of natural remanent magnetization (NRM). Thermomagnetic properties, hysteresis properties, NRM stabilities and the study of fine magnetic structures by north seeking bacteria (NSB) were examined. The sample consists of polycrystalline kamacite, taenite and cloudy taenite, while tetrataenite is absent. The NRM directions scattered widely among subsamples, but each subsample was extremely stable against AF demagnetization up to 100 mT. The S pole alignments observed by NSB were not parallel completely with the crystallographic axis of kamacite. In order to understand the stable NRM of Nova Petrópolis, we must consider the magnetic domains that were reconfigured and stabilized due to deformation by hyper-velocity shocks.

1. Introduction

The iron meteorite Nova Petrópolis weighing 305 kg was found at Nova Petrópolis, Rio Grande do Sul, Brazil, in 1967 (GRUNEWALDT, 1983). Its surface was severely oxidized with up to 3 mm of oxide crust and no trace of fusion crust was recognized. The iron was cut by the authors in order to arrange a sample for exhibit in the museum. A small sample was also obtained at that time for magnetic studies to understand why iron meteorites are magnetized. Although it is suggested that the natural remanent magnetization (NRM) of iron meteorites show insignificant paleomagnetic meaning due to their multi-domain structure, the NRM offers the fundamental data for the signature of magnetic fields associated with the iron type asteroids, and may reveal aspects of the history of iron meteorite magnetic fields, due to crystallization history, heating, strain, and shocks.

Nova Petrópolis has been classified as a medium octahedrite IIIA with chemical composition of 7.8%Ni, 19.9 ppm Ga, 36.5 ppm Ge, 9.4 ppm Ir (GRAHAM *et al.*, 1985). Extracted taenite lamellae resulting from the Widmanstätten structure in this iron were examined by Mössbauer spectroscopy at room temperature (AZEVEDO *et al.*, 1987). The results indicated that the lamellae consist of 15% α-FeNi, 62% Ni rich γ-FeNi, 20% paramagnetic γ-FeNi (<30%Ni), and 3% iron oxide.

NéeL *et al.* (1964) were able to produce a tetragonal structured ordered phase (γ'-phase) by irradiating a man made cubic crystal of 50%Fe50%Ni. The lattice parameters of the tetragonal unit cell (AuCu type) are given as a=2.533Å and c=3.582Å showing

*Deceased October 30, 1989.

therefore the strong magnetic anisotropy supported by the large *Hc* value of about 0.4 T for an assembly of random-oriented crystals. ALBERTSEN *et al.* (1978) found this mineral in chondrites and CLARKE and SCOTT (1980) named it tetrataenite. WASILEWSKI (1982, 1988) elucidated that the stable NRM of chondrites is carried by tetrataenite. The stable NRM of iron meteorites resulting from tetrataenite has been reported from Toluca (group IA, Og; FUNAKI *et al.*, 1986), Ni-rich ataxites (NAGATA *et al.*, 1987) and Bocaiuva (group IAB; FUNAKI *et al.*, 1988). The preliminary report on Nova Petrópolis indicates there is no tetrataenite, nevertheless stable NRM is present, according to FUNAKI (1997). In this study we extend our investigation in order to understand why Nova Petrópolis carries the stable NRM component.

2. Sample Preparation

A total of 9 mutually oriented cubic subsamples (A1-A9), weighing 0.0997–0.1565 g, were obtained from a block sample of Nova Petrópolis. The subsamples A3, A6 and A9 (surface subsample) included a little oxide product due to weathering, but the other subsamples (inner one) did not contain such oxide. Sliced subsamples (B1-B2) were polished with diamond paste and were occasionally etched by nitric acid (5% NO_2-ethyl alcohol) and/or were electropolished. The other subsamples (C1: total 10 g) were etched by hydrochloric acid (HCl) of 1.0 Normal for 10 days. In this treatment kamacite (α-phase) and the low nickel portion of taenite (γ -phase) are attacked severely compared with high nickel portions of taenite. Consequently, Ni-rich taenite lamellae (lamellae sample) and residual powder (residue sample) were extracted in this process.

3. Magnetic Hysteresis Properties

From the hysteresis loop measured at room temperature, using a vibrating sample magnetometer, the basic magnetic properties such as saturation magnetization (I_S), saturation remanent magnetization (I_R), coercive force (H_C), remanent coercive force (H_{RC}) and initial susceptibility (χ_i) were obtained. The values of these magnetic hysteresis properties for the pre- and post-heated samples (850°C in 10^{-3} Pa atmospheric pressure) are summarized in Table 1. The I_S values were calculated by extrapolation of the slope between 1.2 and 1.4 T for the lamellae and residue samples, but they were estimated by extrapolation of the magnetization versus 1/H (reciprocal of the applied field) for the

Table 1. Magnetic hysteresis and thermomagnetic properties.

Sample	Weight (g)	I_S Am²/kg	I_R Am²/kg	H_C mT	H_{RC} mT	χ_i Am²/kg/T	Curie point T_c (°C) Heating	Cooling
Bulk (1st run)	0.03062	207.7	0.175	0.55	51.7	0.032	535, 750	590
(2nd run)		211.5	0.1	0.4	57.7	0.025	750	590
Lamellae (1st run)	0.00124	140	12.2	3.3	7.2	0.370	565, 750	575
(2nd run)		167	1.3	0.2	<1.0	0.650	750	580
Residue (1st run)	0.00643	210	1.4	0.8	10	0.175	750	575
(2nd run)		205	1.1	0.55	1.5	0.200	750	575

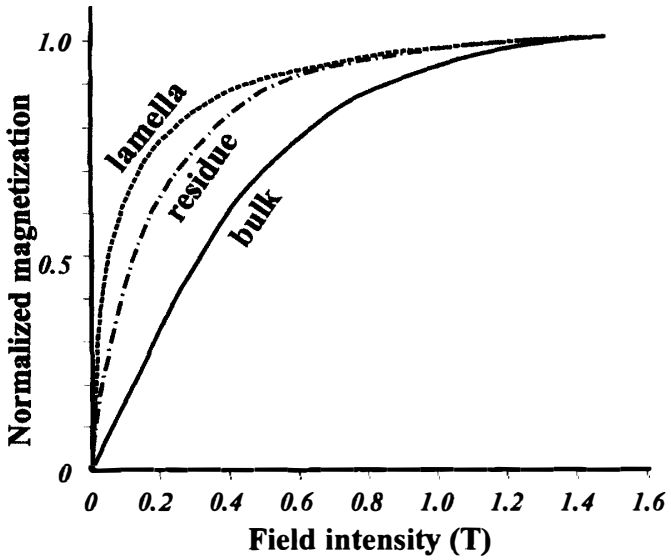

Fig. 1. Magnetization curves of bulk, lamella, and residue samples at room temperature.

bulk sample. The extrapolated magnetization is 200, 139 and 210 Am^2/kg for the bulk, lamellae and residue samples respectively. Normalized magnetization (*M-H*) curves of the samples are shown in Fig. 1. The lamellae and residue samples are almost saturated before 0.2 T, while the bulk sample was not saturated to 1.5 T.

The pre- and post-heating I_S values of the bulk and residue samples are similar to that of the pure iron (217.7 Am^2/kg), whereas the lamellae sample has smaller I_S values as indicated in Table 1. The values of H_C are small for all samples and they decrease following the heat treatment. The H_{RC} value of the bulk sample is larger (H_{RC}=51.7 mT) than other samples (H_{RC} =10 mT), and H_{RC} increase slightly by heating in contrast to the lamellae and residue. Smaller χ_i values characterize the bulk sample compared to lamellae and residue.

4. Thermomagnetic (I_S-T) Curves

Thermomagnetic (I_S-T) curves measured from room temperature to 800°C in a 0.6T magnetic field (under a vacuum of 10^{-3} Pa) were obtained for the bulk, lamellae and residue samples using the vibrating sample magnetometer. The curves of the 1st and 2nd run cycles for the bulk and lamellae samples are illustrated in Fig. 2a and b respectively. The Curie points or phase transition temperatures (T_C) derived from the I_S-T curves are summarized in Table 1.

The I_S-T curve of the bulk sample is reversible with T_c=750° and 590°C in the 1st run cycle and the 2nd run cycle. Observed T_C=750° and 590°C correspond to the phase transition of $\alpha \rightarrow \gamma$ and $\gamma \rightarrow \alpha$ respectively for kamacite with 7%Ni. A Curie point at 535°C is noted in the heating curve (1st run) for the bulk sample, but does not appear in the 2nd cycle. A similar unstable Curie point appeared at 565°C in the lamellar sample. This may be due to some tetrataenite like phase which is decomposed at 535° and 565°C.

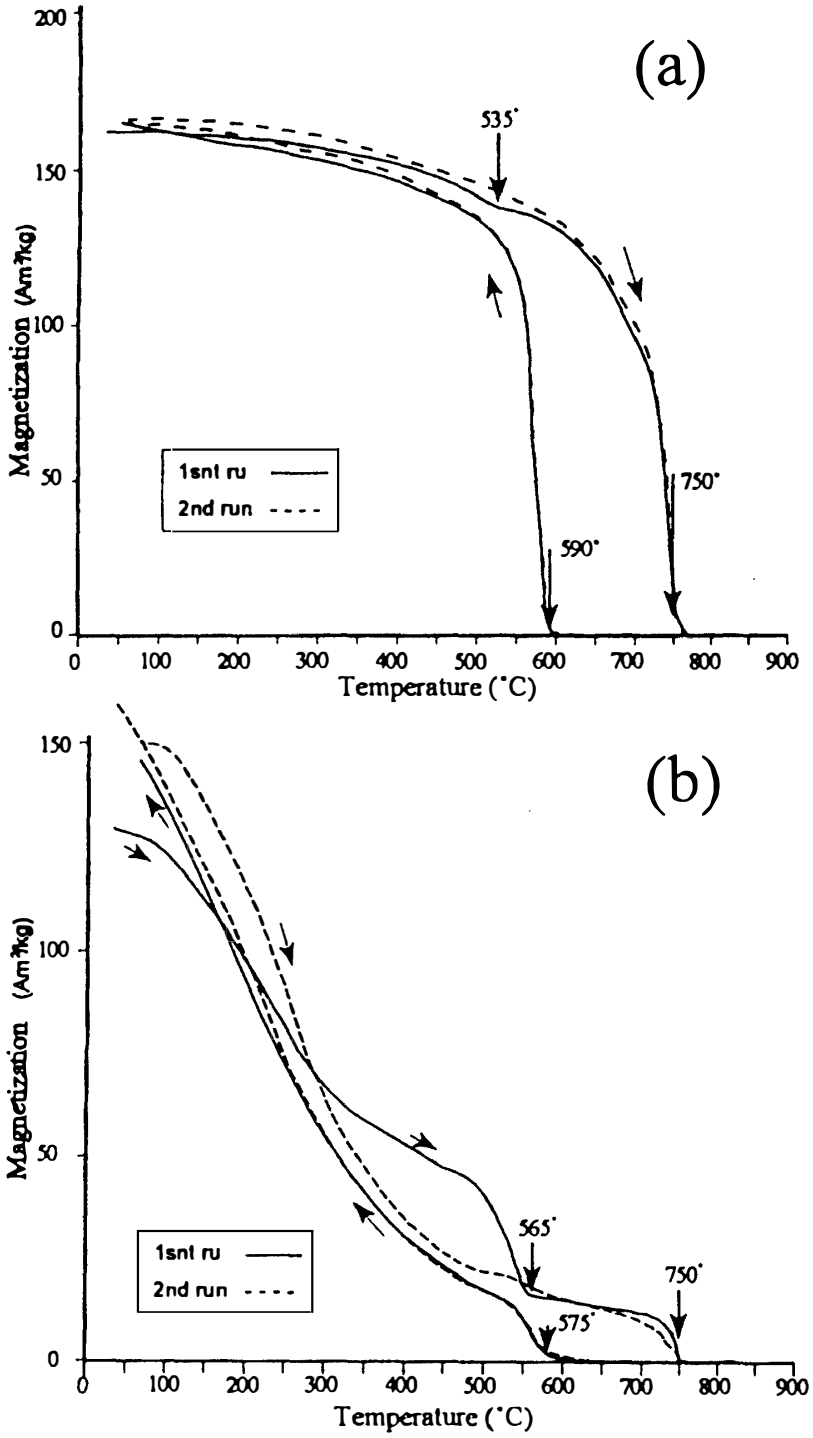

Fig. 2. Thermomagnetic curves (I_S-T) of bulk (a) and lamellae (b) samples obtained in the external magnetic field of 0.6 T and vacuum of 10^{-3}Pa.

However, it may not be well ordered tetrataenite because of the small coercivities, H_C=3.3 mT and H_{RC}=7.2 mT, of the lamellae sample.

5. Natural Remanent Magnetization

Three subsamples (A1, A2, A3) were demagnetized by alternating magnetic field (AF demagnetization) up to 100 mT with a 5 mT interval. Figure 3 shows typical AF demagnetization curves (subsample A1) illustrating intensity change, behavior of vector components (Zjiderveld projection), and the direction (using stereo plot). The NRM

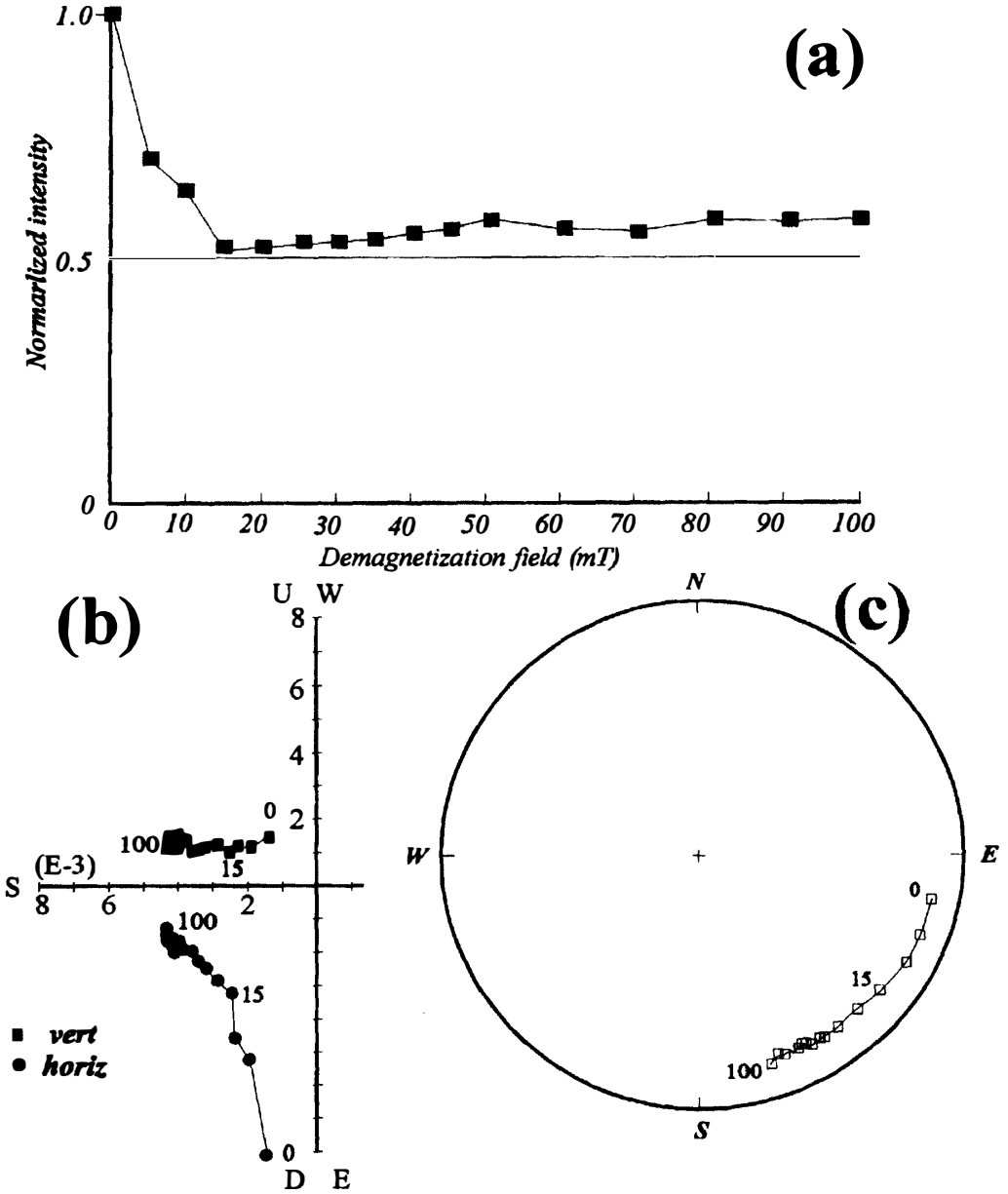

Fig. 3. AF demagnetization curves of NRM for the bulk subsample (A1). (a) intensity change, (b) Zjiderveld projection, (c) direction change.

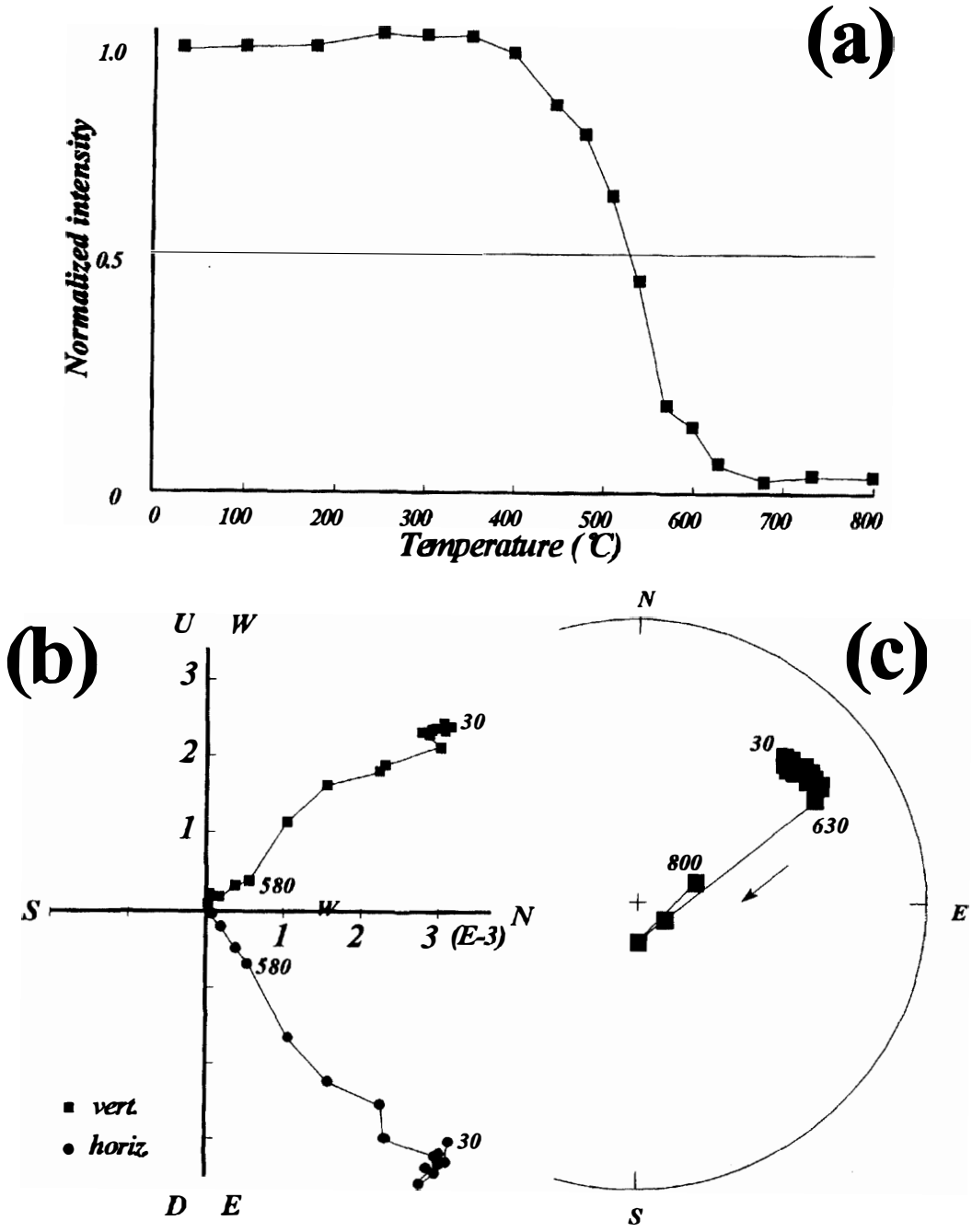

Fig. 4. Thermal demagnetization curves of the stable NRM component (post AF demagnetization to 100 mT) for the bulk subsample (A1). (a) intensity change, (b) Zijderveld projection, (c) direction change.

(8.371×10^{-3}Am^2/kg) is decomposed into soft and hard components at 15 mT in the curves. The intensity of the soft component decayed steeply, while that of the hard one was unchanged up to 100 mT. The direction seems to converge southward throughout the demagnetization. The other 2 subsamples showed almost identical intensity behavior but the convergence points differed.

The hard NRM component of subsample A1, which was demagnetized to 100 mT was then thermally demagnetized up to 800°C (in a vacuum of 10^{-3}Pa atmospheric pressure), as shown in Fig. 4. The demagnetization curve indicates that the intensity ($4.862\times10^{-3}Am^2/kg$) was scarcely demagnetized up to 400°C, and then it demagnetized at first slowly and then steeply from 500° to 580°C. A gradual step from 580° to 630°C indicates the presence of another magnetic carrier. The direction is not changed drastically between 30° to 630°C, subsequently it scatters up to 800°C. These characteristics of thermal demagnetization are essentially consistent with the other 2 subsamples.

The NRM directions, of subsamples A1 to A9, were measured pre- and post-AF demagnetization to 30 mT, as shown in Fig. 5. Circle (inner subsample) and square (surface subsample) symbols denote the upward directions if open , and denote the downward directions if solid. Their NRM intensities range from $1.234\times10^{-2}Am^2/kg$ to $1.551\times10^{-3}Am^2/kg$ for pre-demagnetization and from $4.504\times10^{-3}Am^2/kg$ to 5.436×10^{-3} Am^2/kg for post-demagnetization. The NRM directions of the 6 inner subsamples scatter widely with normal and reverse inclination, while those of the 3 surface subsamples are located at a southward low inclination. These NRM distributions are not changed drastically by AF demagnetization to 30 mT. The surface samples of Nova Petrópolis may be magnetically contaminated by the oxide-metal confluence.

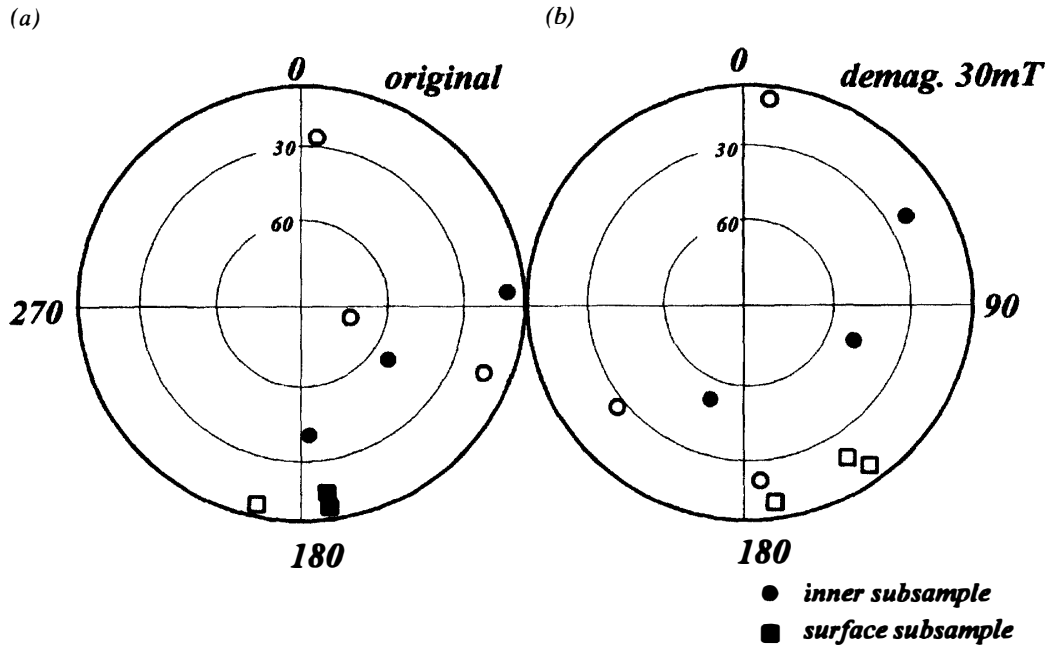

Fig. 5. Directions of NRM of the subsamples for pre- (a) and post-demagnetization (b) to 30 mT. Circles denote inner subsamples and squares denote surface (partially oxidized) ones. Solid (open) symbols denote downward (upward) inclination.

6. Microscopical Observation

The north seeking magnetotactic bacteria (NSB) of cocci type, collected in Tokyo, were cultivated (FUNAKI *et al.*, 1989). They were pipetted with water after enrichment by attraction to the S pole of a small hand magnet. A droplet including numerous NSB was spread on the subsample B1 (after electropolishing). The bacteria migrate toward the S poles formed on the surface along the magnetic field lines. Bacterial clusters of 70×40 μm to 30×20 μm (surrounded by ellipses) appeared, as shown in Fig. 6. In this figure, taenite lamella (L) was sandwiched between 2 kamacite crystals, K1 and K2, and Neumann lines (N) could be seen on K2. The principal axes of the clusters are 210–240° which is similar to the NRM direction (I=11.0°, D=212.7°) of this sample. On the electropolished surface, 2 directions (213° and 303°) of deeper etched linear pits (10–40 μm in length) intersected in perpendicular directions and pits of 5 μm in diameter also appear aligned perpendiclar to these linear pits on K1 (denoted by ↑ in the figure). The pits seems to be cross sections of the linear pits as is most obvious in K2. These linear features may be aligned along the respective crystal axes of kamacite. The maximum axes of the bacterial clusters were not completely parallel or perpendicular to the direction of linear pits in K1, as shown in Fig. 6.

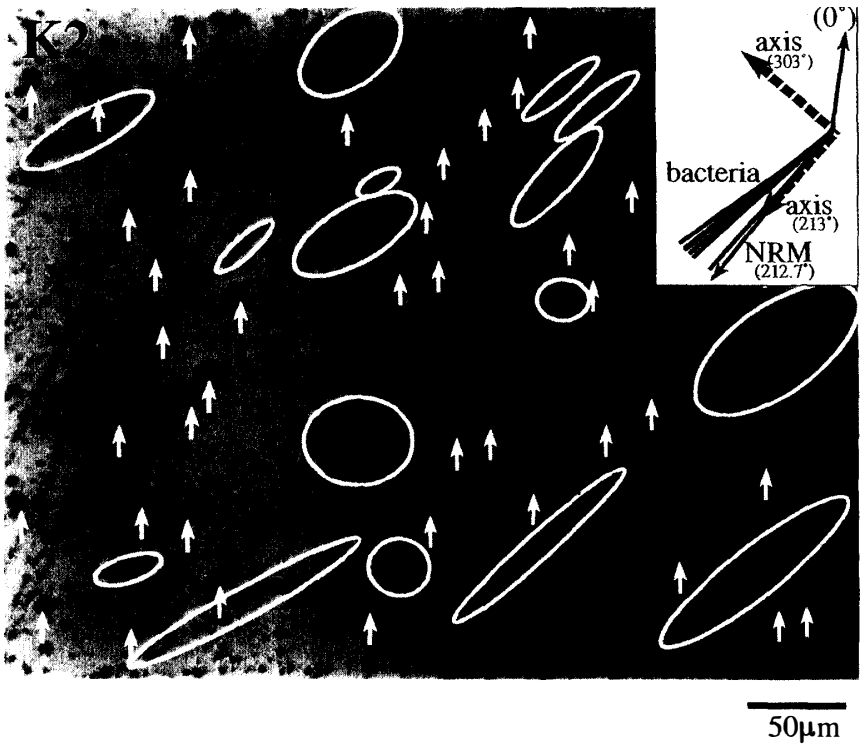

Fig. 6. The S pole distributions observed by north seeking magnetotactic bacteria (NSB) and deeper etched needles of the subsample B1. Ellipse: dominant clusters of bacteria, allows: deeper etched needles by electropolishing, K1 and K2: kamacite crystals, L: taenite lamellae, B: NSB cluster, N: Neumann lines. Upper right: the directions of NRM, maximum axes of bacterial cluster and deeper etched needles.

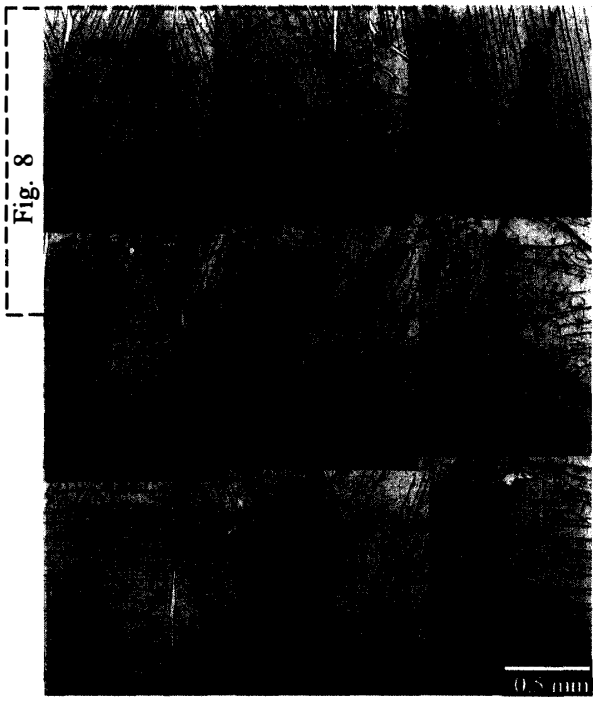

Fig. 7. The representative distribution of crystallites and Neumann lines in the subsample B2 after etching.

An etched surface of subsample (B2), having NRM direction (I=8°, D=282°), was observed with a reflected light microscope, as shown in Fig. 7. The observation indicates that taenite lamellae, less than 100 μm in width, and plessite can be found in the dominant field of polygonal kamacite crystals (0.8 to 4 mm in diameter). Cloudy taenite is seen together with taenite. Profuse parallel sets of Neumann lines with intervals of 10 to 100 μm are developed in all kamacite crystals. The deeper etched linear pits as observed in subsample B1 are also seen in all kamacite fields in Fig. 7. There is no evidence of recrystallization, indicating no significant shock heating. The S pole distribution of this sample was observed by NSB as shown in Fig. 8 (this area is denoted in Fig. 7). The results indicate that parallel alignment of elliptical NSB clusters of 50× 200 μm in size and round ones of ~20 μm in diameter appeared with intervals of 50 to 300 μm. The directions of maximum axes of the elliptical clusters are located at 207, 243, 305 and 319° which is common throughout the kamacite crystals in this sample. The shapes of the clusters may relate to the S pole distribution (FUNAKI *et al.*, 1992); the dominant elliptical clusters may therefore denote an almost horizontal NRM direction inferred from the NRM inclination (I=8°) of this sample. The NRM declination (D=282°) of this sample is, however, not oriented with directions of individual bacterial clusters, as denoted in Fig. 8.

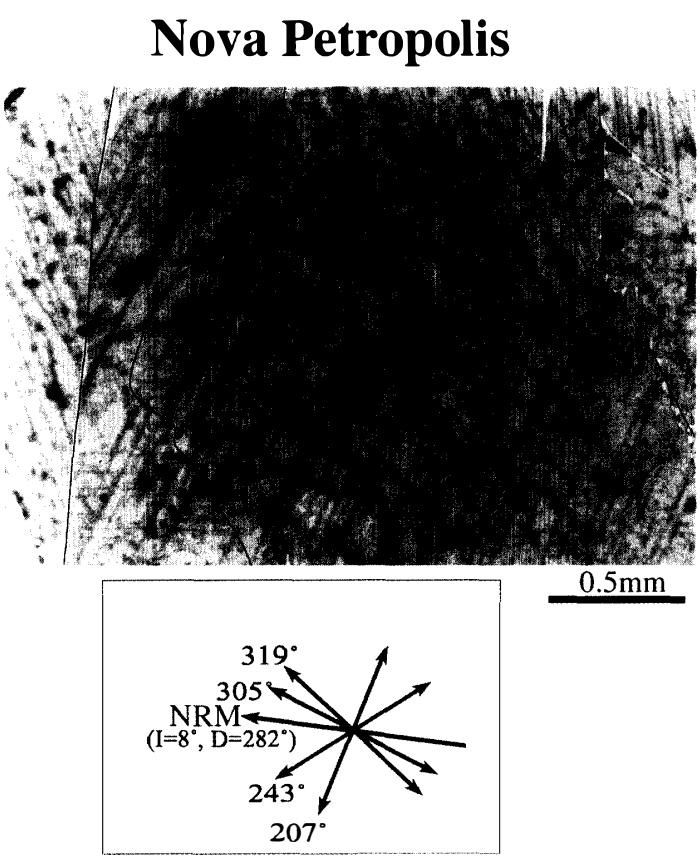

Fig. 8. Typical alignment of the S pole (dark diffuse lines, ellipse, and circle) observed by NSB on the subsample B2. Crystal boundaries are traced by solid lines.

7. Discussion

The main magnetic mineral of Nova Petrópolis is kamacite with 7%Ni identified, by the $\alpha \rightarrow \gamma$ phase transition at 750°C and the $\gamma \rightarrow \alpha$ one at 590°C in the I_S-T curves of the bulk sample (Fig. 2a). This is supported by the chemical analysis (7.8%Ni) reported by GRAHAM *et al.* (1985). The amount of taenite, with T_c=535°C, should be very small compared with kamacite due to the evidence of the small magnetization step in the I_S-T curve. Kamacite in the bulk sample is roughly estimated to be 95.7% based on the I_s=207.7 Am^2/kg of the bulk sample (Table 1) and I_s=217 Am^2/kg of 93%Fe7%Ni (BOZORTH, 1951). This estimation of a large amount of kamacite agrees with the results of microscopical observations. Chemical composition of the lamellae sample cannot easily be identified due to the complicated I_S-T curve (Fig. 2b). This curve should be investigated at cryogenic temperature to characterize this antitaenite, if this is indeed present. RANCOURT and SCORZELLI (1995) proposed nonmagnetic (low-spin γ-FeNi) taenite called "antitaenite" which is often found in taenite lamellae of composition 20–40%Ni associated with the γ'-phase.

Tetrataenite is the most common stable NRM carrier in chondrites and is identified magnetically by the peculiar features of the hysteresis properties and I_S-T curves (WASILEWSKI, 1988); the large coercivity ranging from H_C =30 mT to 600 mT decays rapidly to a few mT associated with the disordering of tetrataenite to taenite at around 550°C. If tetrataenite is included in Nova Petrópolis, this characteristic should appear clearly in the lamellar and residue samples because tetrataenite is resistant to etching due to high Ni content. Actually, tetrataenite (H_C=44.5 mT and H_{RC}=70.4 mT) was extracted from Toluca by this etching technique (FUNAKI *et al.*, 1986). The magnetic properties of the lamellar sample in Nova Petrópolis, however, suggests that tetrataenite is not present due to small H_C=3.3 mT and H_{RC}=7.2 mT values, regardless that the rapid magnetization decay appeared at T_c= 565°C (Fig. 2b). The minerals in the residue sample cannot be identified from the I_S-T curve, but tetrataenite is denied for the same reason. AZEVEDO *et al.* (1987), also, did not detect tetrataenite, in extracted taenite lamellae, by Mössbauer spectroscopy at room temperature. From these viewpoints, the absence of tetrataenite in Nova Petrópolis is considered likely.

If there is no evidence for the existence of tetrataenite in Nova Petrópolis, nevertheless, we must discover why it carries an extremely stable NRM component as observed during AF demagnetization to 100 mT. The stable NRM is considered to be carried by kamacite. This is inferred from the hysteresis properties (relatively large H_C and H_{RC} and small χ_i values) and the NSB patterns (Figs. 6, 8). Deep etched pits observed in kamacite (Figs. 6, 7), after electropolishing, may be sites for stabilization and pinning of domain walls and this would serve to increase magnetic stability. Magnetic contamination of the sample is determined by ratio of NRM to I_R values (REM). If the sample has REM 0.05, generally one must suspect some contamination, perhaps by a hand magnet (WASILEWSKI and DICKINSON, 1998). The REM values for the A1 to A9 subsamples of Nova Petrópolis are between 0.03 and 0.009 for 8 subsamples, although one sample showed REM=0.07 (A2, inner subsample). Thus, these subsamples have NRM's which do not include any large magnetic contaminations. The directions of the stable NRM components among the inner subsamples scattered widely in spite of the high NRM stability. As the NRM's of the surface subsamples (A3,A6,A9) clustered, they might be influenced strongly by oxidation due to weathering, in the earth's magnetic field.

According to the previous studies, clustering of the NRM direction in iron meteorites differs. For example, the NRM directions of Weaver Mountain (Ni-rich ataxite, IVB) clustered, but that of Odessa (coarse octahedrite, Og), and Arizona Craters (probably Canyon Diablo, coarse octahedrite, Og) scattered widely (DUBOIS, 1965). The NRM carrier minerals were considered to be kamacite for Odessa and Arizona Craters and they were studied using the Bitter pattern technique, but all of his results seem to be due to artificial maze-domain structures associated with mechanical strain acquired during polishing. Only one paper described stable NRM directions and identified the carrier minerals; the NRM directions of Bocaiuva (IAB) were aligned along a great circle consistent with the dominant plane of developed tetrataenite lamellae (FUNAKI *et al.*, 1988). Stable NRM carried by kamacite as in Nova Petrópolis has not been reported in iron meteorites.

Neumann lines, shock-produced mechanical twinning lamellae, form along the (211) planes of kamacite at shock pressures of the order of 10 GPa (WASSON, 1974). One of the characteristic features in Nova Petrópolis is the presence of well-developed Neumann lines. They appeared as several sets of parallel lines in a single kamacite crystal, but their directions seem to be differently oriented in many other crystals suggesting the polycrystalline structure. SMITH (1958) reported on the formation of Neumann lines in Armco iron subject to artificial explosive shocks at 13, 14.5, 19, 25 and 60 GPa. The results confirm that shocks below 13 GPa produce only simple Neumann lines.

A large iron mass of kamacite cannot carry the stable NRM due to multidomain structure, nevertheless, Nova Petrópolis carries an extremely stable NRM component in kamacite crystals. As the magnetic easy axis resulting from the crystal anisotropy of kamacite is [100], the magnetic domains with antiparallel directions should be aligned along the preferable directions of crystallographic axes if there is no external magnetic field. In the magnetic field, the domains are aligned toward the axis which is the nearest direction to the magnetic field. In case of Nova Petrópolis, the crystallographic axes and the S pole distribution are not parallel (Fig. 6). This angular deviation may suggest that the NRM was controlled by another factor in addition to the crystal anisotropy. The S pole distributions in Fig. 8 may also be used to suggest the presence of this factor.

In the preliminary study of Nova Petrópolis (FUNAKI, 1997), the NRM carrier was concluded to be associated with Neumann lines because of accumulation of the magnetic fluid (Bitter pattern) along the lines. It now seems likely that the magnetic fluid imaging was dictated by line orientation. In this study, the magnetotactic bacteria did not align along the Neumann lines. Probably the magnetic field lines resulting from Neumann lines close just above the surface, and are not detected at 500 nm above the surface (location of magnetic sensor) by magnetotactic bacteria.

The dominant unblocking temperature of stable NRM for Nova Petrópolis is between 580° and 630°C, but the saturation magnetization decays at 750°C in the I_s-T curves of the bulk sample (Fig. 2). The reason of this inconsistency cannot be explained in this study, but we must consider the temperature dependence of kamacite deformed by hyper-velocity shocks.

8. Conclusion

Nova Petrópolis consists of polycrystalline kamacite with Fe93%Ni7% and is characterized by well-developed Neumann lines, taenite and cloudy taenite, while tetrataenite may not exist. It carries unusual stable NRM against AF demagnetization to more than 100 mT, but the NRM is demagnetized dominantly at 580°C during thermal demagnetization. The NRM directions among subsamples scattered widely, but the oxidized samples clustered due to the remagnetization in the earth's magnetic field. The NRM is carried by kamacite, and the profuse Neumann lines do not directly control the NRM. The S pole alignments observed by NSB are not parallel completely to the crystallographic axis of kamacite. Probably these NRM characteristics may be controlled by the strain distribution in polycrystalline kamacite subject to shock of the order of 10 GPa. Nova Petrópolis may be an example of shock stabilized NRM in kamacite.

Acknowledgments

The authors are indebted to Dr. P. WASILEWSKI, Goddard Space Flight Center, NASA, for constructive suggestions for improving the paper.

References

ALBERTSEN, J.F., JENSEN, G.B. and KNUDSEN, J.M. (1978): Structure of taenite in two iron meteorites. Nature, **273**, 453–454.

AZEVEDO, I.S., SCORZELLI, R.B., DANON, J. and ZUCOLOTTO, M.E. (1987): Mössbauer spectroscopy study of the Nova Petrōpolis meteorite and its corrosion mechanism. Meteoritics, **22**, 320.

BOZORTH, R.M. (1951): Ferromagnetism. New York, D. Van Nastrand, 441 p.

CLARKE, R.S., Jr. and SCOTT, E.R.D. (1980): Tetrataenite-ordered FeNi, a new mineral in meteorites. Am. Mineral., **65**, 624–630.

DUBOIS, R.L. (1965): Some investigations of the remanent magnetism and domain structures of iron meteorites. J. Geomagn. Geoelectr., **17**, 381–390.

FUNAKI, M. (1997): Characteristics of natural remanent magnetization of Nova Petrópolis iron meteorite. Essays on Interdisciplinary Topics in Natural Sciences, ed. by R.B. SCORZELLI *et al.* Paris, Editions Fronteieres, 139–149.

FUNAKI, M., SAKAI, H., MATSUNAGA, T. and HIROSE, S. (1992): The S pole distribution on magnetic grains in pyroxenite determined by magnetotactic bacteria. Phys. Earth Planet. Int., **70**, 253–260.

FUNAKI, M., NAGATA, T. and DANON, J. (1986): Magnetic properties of lamellar tetrataenite in Toluca iron meteorite. Mem. Natl Inst. Polar Res., Spec. Issue, **41**, 382–393.

FUNAKI, M., TAGUCHI, I., DANON, J., NAGATA, T. and KONDO, Y. (1988): Magnetic and metallographical studies of the Bocaiuva iron meteorite. Proc. NIPR Symp. Antarct. Meteorites, **1**, 231–246.

FUNAKI, M., SAKAI, H. and MATSUNAGA, T. (1989): Identification of the magnetic poles on strong magnetic grains from meteorites using magnetotactic bacteria. J. Geomagn. Geoelectr., **41**, 77–87.

GRAHAM, A.L., BEVAN, A.W.R. and HUTCHISON, R. (1985): Catalogue of meteorites. London, British Museum (Natural History) , 246 p.

GRUNEWALDT, H. (1983): Nova Petrópolis: A new Brazilian meteorite from Rio Grande do Sul. An. Acad. Bras. Cienc., **55**, (1), 138–139.

NAGATA, T., DANON, A. J. and FUNAKI, M. (1987): Magnetic properties of Ni-rich iron meteorites. Mem. Natl Inst. Polar Res., Spec. Issue, **46**, 263–282.

NÉEL, L., PAULEVE, J., PAUTHENET, R., LANGIER, J. and DAUTREPPE, D. (1964): Properties of an iron-nickel single crystal ordered by neutron bombardment. J. Appl. Phys., **35**, 873–876.

RANCOURT, D.G. and SCORZELLI, R.B. (1995): Low-spin γ-Fe-Ni (γ_{LS}) proposed as a new mineral in Fe-Ni-bearing meteorites: Epitaxial intergrowth of γ_{LS} and tetrataenite as a possible equilibrium state at ~20–40 at% Ni. J. Magn. Magn. Mater., **150**, 30–36.

SMITH, C.S. (1958): Metallographic studies of metals after explosive shock. Trans. Metall. Soc. AIME, **212**, 574–589.

WASILEWSKI, P. (1982): Magnetic characterization of tetrataenite and its role in the magnetization of meteorite (abstract). Lunar and Planetary Science XIII. Houston, Lunar Planet. Inst, 843–844.

WASILEWSKI, P. (1988): Magnetic characterization of the new magnetic mineral tetrataenite and its contrast with isochemical taenite. Phys. Earth Planet. Int., **52**, 150–158.

WASILEWSKI, P. and DICKINSON, T. (1998): The role of magnetic contamination in meteorites. submitted to Meteorit. Planet. Sci.

WASSON, J. T. (1974): Meteorites. New York, Springer-Verlag, 161 p.

(Received December 1, 1997; Revised manuscript accepted January 28, 1998)